

1 **Title: A large-scale population-based study reveals that gp42-IgG antibody is protective against**  
2 **Epstein-Barr virus-associated nasopharyngeal carcinoma**

3 **Authors:** Xiang-Wei Kong<sup>1, 2†</sup>, Guo-Long Bu<sup>1†</sup>, Hua Chen<sup>1, 13†</sup>, Yu-Hua Huang<sup>1, 12†</sup>, Zhiwei Liu<sup>6</sup>, Yin-  
4 Feng Kang<sup>1, 7</sup>, Yan-Cheng Li<sup>3, 4</sup>, Xia Yu<sup>5</sup>, Biao-Hua Wu<sup>5</sup>, Zi-Qian Li<sup>1</sup>, Xin-Chun Chen<sup>1</sup>, Shang-Hang  
5 Xie<sup>1</sup>, Dong-Feng Lin<sup>1</sup>, Tong Li<sup>1</sup>, Shu-Mei Yan<sup>1, 12</sup>, Run-Kun Han<sup>1</sup>, Nan Huang<sup>1</sup>, Qian-Yu Wang<sup>11</sup>, Yan  
6 Li<sup>1, 12</sup>, Ao Zhang<sup>1</sup>, Qian Zhong<sup>1</sup>, Xiao-Ming Huang<sup>2</sup>, Weimin Ye<sup>8, 9, 10</sup>, Ming-Fang Ji<sup>5\*</sup>, Yong-Lin Cai<sup>3, 4\*</sup>,  
7 Su-Mei Cao<sup>1\*</sup>, Mu-Sheng Zeng<sup>1\*</sup>

8 **Affiliations:**

9 <sup>1</sup>State Key Laboratory of Oncology in South China, Collaborative Innovation Center for Cancer  
10 Medicine, Guangdong Key Laboratory of Nasopharyngeal Carcinoma Diagnosis and Therapy, Sun  
11 Yat-sen University Cancer Center (SYSUCC), Guangzhou, Guangdong, China.

12 <sup>2</sup>Department of Otorhinolaryngology, Sun Yat-sen Memorial Hospital, Sun Yat-sen University,  
13 Guangzhou, Guangdong, China

14 <sup>3</sup>Guangxi Health Commission Key Laboratory of Molecular Epidemiology of Nasopharyngeal  
15 Carcinoma, Wuzhou Red Cross Hospital, Wuzhou, Guangxi, China.

16 <sup>4</sup>Department of Preventive Medicine, Wuzhou Cancer Center, Wuzhou, Guangxi, China.

17 <sup>5</sup>Cancer Research Institute of Zhongshan City, Zhongshan City People's Hospital, Zhongshan,  
18 Guangdong, China.

19 <sup>6</sup>Division of Cancer Epidemiology and Genetics, National Cancer Institute, Rockville, Maryland,  
20 USA.

21 <sup>7</sup>Guangdong Provincial People's Hospital, Guangdong Academy of Medical Sciences, Guangzhou,  
22 Guangdong, China.

23 <sup>8</sup>Department of Epidemiology and Health Statistics, School of Public Health, Fujian Medical  
24 University, Fuzhou, Fujian, China.

25 <sup>9</sup>Key Laboratory of Ministry of Education for Gastrointestinal Cancer, Fujian Medical University,  
26 Fuzhou, Fujian, China.

27 <sup>10</sup>Department of Medical Epidemiology and Biostatistics, Karolinska Institutet, Stockholm, Sweden.

28 <sup>11</sup>Key Laboratory of Carcinogenesis and Translational Research (Ministry of Education/Beijing),  
29 Laboratory of Molecular Oncology, Peking University Cancer Hospital & Institute, Beijing, China.

30 <sup>12</sup>Department of pathology, Sun Yat-sen University Cancer Center (SYSUCC), Guangzhou,  
31 Guangdong, China.

32 <sup>13</sup>Zhongshan School of Medicine, Sun Yat-sen University, Guangzhou, Guangdong, China.

33 #Address correspondence to Prof. Mu-Sheng Zeng: Sun Yat-sen University Cancer Center, 651  
34 Dongfengdong Avenue, Guangzhou, Guangdong, China. Mail stop code: 510060. Phone number: +86-  
35 20-87343192. Email: zengmsh@sysucc.org.cn (M.-S.Z.).

36 #Address correspondence to Prof. Su-Mei Cao: Sun Yat-sen University Cancer Center, 651  
37 Dongfengdong Avenue, Guangzhou, Guangdong, China. Mail stop code: 510060. Phone number: +86-  
38 20-87345685. Email: caosm@sysucc.org.cn (S.-M.C.).

39 #Address correspondence to Prof. Yong-Lin Cai: Wuzhou Red Cross Hospital, #3-1, Xinxing Yi Road,  
40 Wuzhou, Guangxi, China. Mail stop code: 543002. Phone number: +86-774-3849595. Email:  
41 cylzen@163.com.

42 #Address correspondence to Prof. Ming-Fang Ji, Cancer Research Institute of Zhongshan City,  
43 Zhongshan City People's Hospital, Zhongshan, Guangdong, China. Mail stop code: 528404. Phone  
44 number: +86-760-89880417. Email: jmftbh@sina.com.

45 †X.-W.K., G.-L.B., H.C., and Y.-H.H. were co-first authors.

46 The authors have declared that no conflict of interest exists.

47

48 **Abstract**

49 **Background**

50 Epstein-Barr virus (EBV) is associated with nasopharyngeal carcinoma (NPC), but the existence of NPC  
51 protective antibody against EBV-associated antigens remains inconclusive.

52 **Methods**

53 NPC cases and matched controls were identified from prospective cohorts comprising 75,481 participants  
54 in southern China. ELISA and conditional logistic regression were applied to assess effects of gp42-IgG  
55 on NPC. The expression of HLA-II, the gp42 receptor, in nasopharyngeal atypical dysplasia and its  
56 impact on EBV infecting epithelial cells were evaluated.

57 **Findings**

58 gp42-IgG titers were significantly lower in NPC cases compared to controls across various follow-up  
59 years before NPC diagnosis ( $P < 0.05$ ). Individuals in the highest quartile of gp42-IgG titers had a 71%  
60 NPC risk reduction comparing to those in the lowest quartile (odds ratios [OR]<sub>Q4vsQ1</sub>=0.29, 95%  
61 confidence intervals [CIs]=0.15 to 0.55,  $P < 0.001$ ). Each unit antibody titer increase was associated with  
62 34% lower risk of NPC (OR=0.66, 95% CI=0.54 to 0.81,  $P_{\text{trend}} < 0.001$ ). Their protective effect was  
63 observed in cases diagnosed  $\geq 5$  years, 1-5 years and  $< 1$  year after blood collection ( $P < 0.05$ ). HLA-II  
64 expression was detected in 13 of 27 nasopharyngeal atypical dysplasia and its overexpression  
65 substantially promoted epithelial-cell-origin EBV infection.

66 **Conclusion**

67 Elevated EBV gp42-IgG titers can reduce NPC risk, indicating gp42 as a potential EBV prophylactic  
68 vaccine design target.

69 **Trial registration**

70 NCT00941538, NCT02501980, ChiCTR2000028776, ChiCTR2100041628.

71 **Funding**

72 Noncommunicable Chronic Diseases-National Science and Technology Major Project, National Natural  
73 Science Foundation of China, Local Innovative and Research Teams Project of Guangdong Pearl River  
74 Talents Program, Central Financial Transfer Payment Projects of the Chinese Government, Cancer  
75 Research Grant of Zhongshan City.

76

77 **Main text**

78 **Introduction**

79 The incidence of nasopharyngeal carcinoma (NPC) demonstrates a striking geographical variation (1). In  
80 endemic regions such as southern China, the age-adjusted incidence can reach 23/100,000 in males and  
81 7/100,000 in females, which is 10-fold higher than the global incidence (2). The regional variation implies  
82 a complex interplay of genetic predisposition, environmental risk factors, and notably, Epstein-Barr virus  
83 (EBV) infection (1, 3).

84 In endemic regions, where over 95% of NPC cases can be attributed to EBV infection, there is a great  
85 opportunity for prevention interventions via EBV vaccination to reduce NPC burden. However, a major  
86 obstacle emerges when selecting an optimal target for vaccine design, considering as many as five surface  
87 glycoproteins with definitive functions that EBV expresses (4). Glycoproteins gB, gHgL, and gp350 have  
88 been spotlighted in the development of EBV prophylactic vaccines due to their pivotal roles in EBV-host  
89 interactions (4), availability of potent monoclonal antibodies against them (5-8), and encouraging results  
90 from preliminary lab-based trials (9). Nonetheless, initial studies assessing neutralizing antibodies  
91 targeting gp350 in three cohorts with modest sample sizes have shown inconsistent results, with one  
92 showing an association with reduced NPC risk (10), while the other two found associations with  
93 increased NPC risk (11, 12). In our previous nested case-control study from a community-based NPC  
94 screening cohort, we also tested antibodies against gp42, gHgL, gB, and gp350, as well as B cell and  
95 epithelial cell neutralizing antibodies. Our results suggest a potential protective role for antibodies against  
96 gp42, with gp42-IgG showing a stronger correlation with epithelial and B cell neutralization competence  
97 compared to gp42-IgA. However, the evidence remains inconclusive, partly due to the limited sample size  
98 (20 cases and 40 controls) (13). It is worth noting that vaccines aiming at gp42 have been less studied  
99 (14).

100 To follow-up on our initial findings, here, we conducted a larger nested case-control study utilizing  
101 samples from 129 NPC cases and 387 matched controls, which were collected prospectively across three

102 independent cohorts in southern China independent from our previous study (13). Our findings confirmed  
103 the inverse association between increased levels of anti-gp42 antibodies and NPC risk. In addition, we  
104 sought to explore the physical and molecular basis by examining the presence of HLA-II, the only known  
105 receptor for gp42, in nasopharyngeal atypical dysplasia samples. This analysis showed that  
106 overexpression of HLA-II in epithelial cells promotes EBV infection. Taken together, our findings  
107 suggest that IgG antibodies against gp42 play a protective role against NPC in endemic regions, thereby  
108 marking gp42 as a potential prophylactic vaccine design target to prevent NPC in high-risk populations.  
109

## 110 **Results**

### 111 **Study population**

112 Based on three prospective community-based cohorts in Sihui, Wuzhou and Zhongshan cohorts with a  
113 total 75,481 individuals, we conducted a nested case-control study to assess whether elevated levels of  
114 gp42-IgG are associated with lower risks of NPC. Blood samples from 129 NPC cases and 387  
115 individually matched controls at 1:3 ratio by age, sex, blood collection time and region were obtained  
116 with a median of 1.3 years (IQR=0.3-2.9 years) before NPC diagnosis (Figure 1). Characteristics of the  
117 NPC cases and controls included in the analysis were shown in Table 1. A majority of participants were  
118 male (76.0%) and at ages of 50-59 years at baseline (44.2%), and NPC cases were more likely to have a  
119 higher EBV-antibody based risk score compared to controls. A longer follow-up duration was observed  
120 for those in the Zhongshan cohort ( $P<0.001$ ) (Supplemental Figure 1). All samples were independent  
121 from our previous study (13).

### 122 **Elevated gp42-IgG titers in disease-free controls comparing with incident NPC cases**

123 To accurately quantify serum levels of gp42-IgG and make comparison in different batches of samples,  
124 we developed an ELISA detection system and assessed the linearity and precision using serial dilution of  
125 monoclonal human gp42 antibody in house. The ELISA showed excellent linearity (goodness of fit of  
126 least square regression  $R^2=0.95$ ) over a broad dynamic range of 0.46–111 ng/mL (Supplemental Figure  
127 2A). We demonstrated the reproducibility by repeating measurements on the three concentrations of  
128 monoclonal gp42 antibody standards in triple and across 11 batches. Results showed CVs of less than  
129 20% (Supplemental Figure 2B; Supplemental Table 1), with the corresponding Inter-ICC of 0.97 (95%CI:  
130 0.92-0.97) and Intra-ICC of 0.92 (95%CI: 0.43-0.99) For the randomly selected 10% serum samples  
131 ( $n=52$ ), the results showed a 5% CV for the duplicated testing samples.

132 Notably, gp42-IgG titers were significantly lower in NPC cases compared to the controls in the overall  
133 cohort ( $P<0.001$ ), and in subgroups with follow-up  $\leq 1$  year ( $P=0.008$ ), 1-5 years ( $P=0.007$ ), and  $\geq 5$  years



134 ( $P=0.027$ ) before NPC diagnosis (Figure 2). However, the overall distribution of gp42-IgG titers  
135 remained consistent across sexes ( $P=0.174$ ), age groups ( $P=0.320$ ) (Supplemental Figure 3). To evaluate  
136 the associations of gp42-IgG titer with NPC risk score, we analyzed the gp42-IgG titers at various EBV  
137 antibody NPC risk scores in controls by different follow-up durations. Result showed that the controls  
138 with low-risk score were more likely to have higher gp42-IgG titers compared to those with medium- and  
139 high-risk scores in the overall cohort ( $P<0.001$ ), and the subgroups with  $\leq 1$  year ( $P=0.051$ ), 1-5 years  
140 ( $P<0.001$ ), and  $\geq 5$  years ( $P=0.212$ ) follow-up before NPC diagnosis (Supplemental Figure 4).

#### 141 **The risk of NPC is the highest in individuals with the lowest gp42-IgG titers**

142 We categorized individuals into quartiles based on gp42-IgG levels in controls and explored the  
143 association between gp42-IgG levels and NPC risks using conditional logistic regression. We found that  
144 in the overall cohort, elevated levels of gp42-IgG in the highest quartile reduced 71% NPC risk (odds  
145 ratios [OR] $_{Q4vsQ1}=0.29$ , 95% CI $_{Q4vsQ1}=0.15$  to  $0.55$ ) and the risks of NPC decreased as the levels of gp42-  
146 IgG increased ( $P_{trend}<0.001$ ). When stratified by length of follow-up, the inverse association with dose-  
147 response trend persisted among cases diagnosed  $\leq 1$ , 1-5, and  $\geq 5$  years after blood collection, with the  
148 corresponding OR $_{Q4vsQ1}$  of 0.33, 0.33, and 0.05, respectively and all the  $P_{trends}<0.05$  (Table 2). The inverse  
149 associations could be consistently observed among the subgroups with different sexes, ages, cohorts, and  
150 EBV-antibody NPC risk scores, with all the  $P_{heterogeneity}\geq 0.05$  (Supplemental Figure 5).

#### 151 **Expression of HLA-II, the sole identified gp42 receptor, is detectable in nasopharyngeal atypical** 152 **dysplasia**

153 The expression of HLA-II is notably detectable in NPC tumor cells (15); however, it remains unclear  
154 whether the expression of HLA-II precedes tumor occurrence. To address this hypothesis, we collected 27  
155 nasopharyngeal premalignant tissues from Sun Yat-sen University Cancer Center, China, where samples  
156 underwent examination by two experienced pathologists independently. Among the 27 premalignant

157 samples, 20 were positive for EBERs, 13 were positive for HLA-DRA, and 12 were positive for both  
158 HLA-DRA and EBERs (Supplemental Table 2; Figure 3; Supplemental Figure 6).

### 159 **HLA-II facilitates epithelial-origin EBV infection of epithelial cells**

160 To further investigate the functional implications of HLA-II expression in epithelial cells, we established  
161 stable HEK293 and NP69 cell lines overexpressing HLA-DRA/DRB. The overexpression of HLA-DR  
162 had a notable impact on enhancing the infection of CNE2-EBV, the representative of EBV originating  
163 from epithelial cells (Supplemental Figure 7, A and C; Supplemental Figure 8, A and C). However, this  
164 effect was only marginal in promoting the infection of Akata-EBV, the representative of EBV originating  
165 from B cells (Supplemental Figure 7, B and D; Supplemental Figure 8, B and D).

166 To further validate the role of gp42 in mediating CNE2-EBV infection, we purified soluble gp42 and  
167 HLA-DRA/DRB. Treating cells with soluble gp42 and HLA-DRA/DRB led to a dose-dependent  
168 inhibition of EBV infection (Supplemental Figure 9, A and B). Interestingly, the inhibitory effects were  
169 countered by the overexpression of HLA-DRA/DRB (Supplemental Figure 7, E and F; Supplemental  
170 Figure 9, C and D). Overexpression of HLA-DRA/DRB was confirmed through western blot analysis  
171 (Supplemental Figure 7G). These results strongly suggest that gp42 plays an important role in promoting  
172 the infection of EBV originating from epithelial cells into HLA-DR-expressing epithelial cells.

173

174 **Discussion**

175 We have conducted the largest, prospective epidemiological study to date, focusing on NPC-associated  
176 protective antibodies against EBV based on three mass screening cohorts. Our findings establish the  
177 protective capacity of gp42-IgG against NPC in endemic regions. Moreover, our research has elucidated  
178 the underlying mechanistic foundations of these protective effects. The identification of HLA-II, the sole  
179 receptor for gp42, in nasopharyngeal atypical dysplasia constitutes a novel discovery. Our experiments  
180 have further demonstrated that the overexpression of HLA-II amplifies the infectivity of EBV within  
181 epithelial cells. Our results on the interplay between gp42-IgG, HLA-II, and EBV infection offer valuable  
182 insights for the mechanisms of the observed gp42-IgG protective effects against NPC.

183 Previous studies have shown that the elevation of antibodies against EBV EA, EBNA1, and VCA are  
184 associated with a higher risk of NPC, which leads to utilization the EBV-associated antibodies as the  
185 screening markers for NPC in endemic regions (16). In comparison with these markers, the precise roles  
186 of antibodies against glycoproteins in the development of NPC remain inconclusive. Although gB, gHgL,  
187 and gp350 play essential roles in EBV infection cells, antibodies targeting these components do not  
188 exhibit significant protective effects against NPC development, as demonstrated in previous studies (11-  
189 13). In this study, which encompassed 129 incident NPC cases and 387 matched controls, we established  
190 statistically significant reduction in NPC risks among cases overall and diagnosed  $\leq 1$  year, 1-5 years,  $\geq 5$   
191 years after blood collection with dose-response trends. Moreover, the protective effects of gp42-IgG can  
192 be observed across varying sexes, age groups, and cohorts, indicating the robustness of the protective  
193 influence of gp42-IgG against NPC. However, in the previous report, gp42-IgG levels were nominally  
194 higher in controls than in those who developed NPC more than 5 years post-collection, but lower in  
195 controls than in those who developed NPC within 5 years (12). This discrepancy could be due to the  
196 differences in antigenicity and measurement methods. In terms of antigenicity, our purified gp42 can  
197 substantially block EBV entry in epithelial cells (Supplemental Figures 7F, 9B, 9D), which was not tested  
198 previously (12), and our purified gp42 was used to identify two potent EBV-neutralizing antibodies (17).

199 In terms of measurement methods, we applied ELISA versus the high-throughput Luminex assay in the  
200 previous report (12).

201 Notably, gp42 is recognized as a crucial molecule that dictates the host preference of EBV (18). A higher  
202 presence of gp42, released through epithelial cell lytic infection, results in a preference for B cell  
203 infection due to the expression of HLA-II by B cells rather than epithelial cells under physiological  
204 conditions. Our research shows that the overexpression of HLA-II only minimally promotes the infection  
205 of B-cell-origin EBV in epithelial cells. This observation prompted us to speculate whether, in  
206 physiological settings, while antibodies against gB, gHgL, and gp350 confer a foundational level of  
207 humoral protection against EBV infection and reactivation, the continuous exposure of epithelial-cell-  
208 origin EBV in nasopharyngeal niches might warrant higher titers of gp42 antibodies. Such elevated titers  
209 could counteract the susceptibility of nasopharyngeal premalignant lesions to epithelial-cell-origin EBV  
210 infection, thereby diminishing the risk of NPC development.

211 Direct evidence concerning the origin of EBV driving NPC remains elusive. Nevertheless, recent studies  
212 indicate persistent exposure to epithelial-cell-origin EBV in nasopharyngeal niches. First, with regard to  
213 Cp methylation percentage of the EBV genome, methylation levels are notably lower in lytic infection  
214 than in latent infection (19); furthermore, evidence suggests that EBV DNA can be detected in  
215 nasopharyngeal swabs as early as three years before NPC development (20). When compared with  
216 healthy controls, nasopharyngeal swabs from NPC patients exhibit significantly higher Cp methylation  
217 percentages of EBV DNA (21). Second, considering gp42, the quantity of surface-bound gp42 on EBV  
218 serves as an indirect indicator of its origin. HLA-II expressed in B cells can capture and reduce the  
219 amount of surface-bound gp42 on released EBV (18). Evidence demonstrates that saliva-origin EBV  
220 possesses significantly higher levels of gp42 when compared with EBV originating from LCLs (22).  
221 Third, with respect to EBV release rate, studies have proposed that the primary source of EBV in saliva is  
222 epithelial lytic infection, as the release rate far surpasses that of the maximum release rate from the  
223 pharyngeal lymphatic ring (23). Lastly, in immune-competent healthy populations, EBV lytic infection

224 can be detected in the parotid gland and the tongue's edge (24, 25). Collectively, these findings suggest  
225 constant exposure of epithelium-origin EBV in nasopharyngeal niches. Consequently, elevated levels of  
226 antibodies against gp42 hold the potential to reduce the likelihood of EBV infection within these niches.  
227 In our recent study, we have identified two human monoclonal antibodies against gp42, named 2C1 and  
228 2B7, bearing strong neutralizing effect against epithelial-cell-origin EBV infecting epithelia, the NOK  
229 cell line (IC50=0.091 and 0.022  $\mu\text{g}/\text{mL}$ , respectively), which provide another strong evidence on the NPC  
230 protective effects of gp42-IgG (17).

231 Though we have provided compelling evidence on the NPC protective role of gp42-IgG, some limitations  
232 require further exploration. First, the median observation period is 1.3 years, indicating a possible reverse  
233 causality, but our results still demonstrated a significant NPC-risk reduction in the individuals with  $\geq 5$   
234 years follow-up period after blood collection should alleviate the concern. Second, the protective effects  
235 on gp42-IgG in less prevalent regions remain elusive, and the correlation between gp42-IgG and other  
236 NPC risk factors, such as genetic predisposition and environmental factors, requires further exploration  
237 (1, 3). Finally, while we have proposed that HLA-II expression in premalignant nasopharyngeal dysplasia  
238 may account for the protective role of gp42-IgG, it is still unclear how gp42-IgG levels relate to HLA-II  
239 expression levels in nasopharyngeal tissue, when and how HLA-II expression is initiated, and how EBV  
240 infection in HLA-II-expressing premalignant nasopharyngeal dysplasia leads to malignant transformation.

241 In conclusion, our proposal posits that the expression of HLA-II in nasopharyngeal atypical dysplasia  
242 predisposes EBV infection originating from the nasal cavity, pharynx, and oral cavity. This susceptibility  
243 can be efficiently countered by high levels of gp42-IgG, decreasing the risk of NPC development.  
244 Accordingly, prioritizing gp42-targeting EBV vaccines in high-risk populations appears warranted to  
245 mitigate NPC risk.

246

247 **Methods**

248 **Sex as a biological variable**

249 Our study examined male and female, and similar findings were reported for both sexes.

250 **Prospective NPC screening cohorts**

251 This study was nested within three large-scale population-based screening trials, conducted in Sihui city  
252 and Wuzhou city for NPC screening, and Zhongshan city for liver cancer screening in southern China (20,  
253 26). Between 2014 and 2018, 30,038 local residences aged 30-69 years were recruited in Sihui city and  
254 followed up until 2023; between 2018 and 2021, 27,477 residences aged 30-69 years were recruited in  
255 Wuzhou city and followed-up until 2023; and in 2012, 17,966 residences aged 35-64 years were recruited  
256 in Zhongshan city until follow-up 2022. In Sihui and Wuzhou cohorts, baseline serum was tested for the  
257 screening markers of EBV VCA/EBNA1-IgA by ELISA with commercial detection kit (EUROIMMUN  
258 AG, Lübeck, Germany, and Zhongshan Bio-Tech Company, Zhongshan, China, respectively). NPC risk  
259 scores of each participant are determined by the risk prediction algorithm ( $\text{Logit } P = -3.934 + 2.203 \times \text{VCA-}$   
260  $\text{IgA} + 4.797 \times \text{EBNA1-IgA}$ ) and stratified by the P scores (Low risk,  $P < 0.65$ ; Medium risk,  $0.65 \leq P < 0.98$ ;  
261 High risk,  $P \geq 0.98$ ) (26). For individuals with low and medium NPC risk scores, EBV antibody retesting  
262 is conducted in every 5- and 1-years intervals, while the high-risk individuals are referred to  
263 nasopharyngeal endoscopy and pathological biopsy will be performed if suspicious lesions are found. In  
264 all the three cohorts, the baseline blood components (plasma, serum, and white blood cells) were  
265 separated within 4-6 hours post collection and stored at  $-80^{\circ}\text{C}$  for future research. The preserved baseline  
266 serum samples were used for gp42-IgG testing for the whole individuals in the nested case-control study,  
267 and for VCA-IgA, and EBNA1-IgA testing in Zhongshan cohort. NPC cases were identified through local  
268 cancer and death registration system in Zhongshan cohort, as well as in the Sihui and the Wuzhou  
269 cohorts.

270 The median follow-up period were 1·2 years (IQR=0.3-2.7 years), 0·6 years (IQR=0.3-1.5 years), and 3·6  
271 years (IQR=2.2-5.2 years) in the Sihui cohort, the Wuzhou cohort, and the Zhongshan cohort and 81, 27,  
272 and 34 incident NPC cases were identified, correspondingly. However, the serum of 13 cases in  
273 Zhongshan cohort are unavailable. Thus, a total of 129 incident NPC cases and 387 controls were  
274 matched with a 1:3 ratio by sex, age (<40, 40 to 50, 50 to 60, ≥60 years old), sample collection date (±6  
275 months), and regions. Race and ethnicity were not considered a variable in this study.

### 276 **Soluble protein purification**

277 Soluble EBV (strain M81) glycoproteins gp42 and HLA-DR were purified by 293F protein expression  
278 system cultured with chemically defined medium (UP1000, Union Bio) under CO<sub>2</sub> supplied shaking  
279 incubator. Transmembrane and cytoplasmic parts of them were truncated for the expression of soluble  
280 proteins, signal peptides were optimized for higher yield, and the His-tag was appended to the C-  
281 terminus. Six to seven days post transfection, supernatant was collected and purified with Ni Sepharose  
282 excel (17371202, Cytiva). Eluate was further purified by Superdex 200 Increase 10/300 GL (28990944,  
283 Cytiva). Protein concentration was determined by the BCA method (23225, Pierce). Protein was  
284 aliquoted, frozen with liquid N<sub>2</sub>, and stored at -80°C for further use.

### 285 **Enzyme-link immunosorbent assay (ELISA)**

286 One hundred nanogram of soluble proteins were added to 96-well plates with high binding surface  
287 followed by overnight incubation at 4 °C. Supernatant was discarded and 5% BSA in PBST (T stands for  
288 0·1% Tween-20) was added to block non-specific binding followed by 1 hour incubation at 37 °C.  
289 Supernatant was discarded. Plates were washed 1 time with PBST. Serums were diluted to 60 folds with  
290 5% BSA in PBST, and then added to 96-well plates followed by 1 hour incubation at 37 °C. Plates were  
291 washed 3 times with PBST. Anti-human IgG was diluted at a ratio of 1:5,000 with 5% BSA in PBST and  
292 added to each well followed by 1 hour incubation at 37 °C. Plates were washed 3 times with PBST. TMB  
293 (PA107-02, TIANGEN) substances were added to each well. Reactions were developed at room  
294 temperature for 10 mins and stopped by adding 1:12 diluted HCl. Read plates at OD450 and OD630. In

295 each 96-well plate, two wells were set to be negative controls (NCs), where no serum was added; seven  
296 wells contain serially diluted monoclonal gp42-IgG. Then, we derive rOD from the following equations:  
297 
$$\frac{((\text{OD}_{450}-\text{OD}_{630})-\text{average}(\text{OD}_{450}-\text{OD}_{630} \text{ of NCs}))}{((\text{OD}_{450}-\text{OD}_{630} \text{ of the highest}$$
  
298 
$$\text{concentration monoclonal anti-gp42})-\text{average}(\text{OD}_{450}-\text{OD}_{630} \text{ of NCs}))}.$$

### 299 **Randomization and masking**

300 Using a random number generator, samples from cases and controls by cohort were randomly assigned to  
301 each ELISA plate in a 1:3 allocation. The testing operators were blinded to the serum origination from  
302 cases or controls and the data were pooled by independent data monitoring staff for statistical analyses.

### 303 **Linearity and precision assessment**

304 Linearity was assessed using serial dilution of standard monoclonal human gp42 antibody in house. After  
305 serial three-fold dilution of the antibody with the initial concentration of 1,000 ng/mL, 8 samples ranging  
306 from 0.46 ng/mL to 1,000 ng/mL were tested in triplicate and simulated (17, 27). To assess within plate  
307 and across plate variation, three concentrations of gp42-IgG standards (1,000 ng/mL, 37 ng/mL, 12.3  
308 ng/mL) were tested in triple in one plate and across 11 batches. Inter- and intra-plate variances and  
309 agreements were assessed using the coefficient of variation (CV) and intraclass correlation coefficients  
310 (ICC) (28). In addition, 10% of the serum samples were randomly selected for duplicate testing in each  
311 plate to further evaluate the precision of gp42-IgG. A standardized value (rOD)—the mean of duplicate  
312 testing, were used for statistical analysis.

### 313 **EBV virion preparation**

314 In this study, Akata strain EBV virions were prepared from CNE2-EBV cell strains and Akata-EBV cell  
315 strains, where the former and the latter represent epithelium- and lymphocyte-origin EBV. Preparation of  
316 these virions followed previous reports (15). Here, we briefly described the virion preparation process.

317 For epithelium-origin EBV preparation, CNE2-EBV cell strains were cultured in RPMI 1640  
318 (C11875500BT, Gibco) supplied with 10% fetal bovine serum (FSP500, ExCell Bio). When cells reached



319 80% confluency, TPA (50601ES03, YEASEN) and NaB (B5887-1G, Sigma-Aldrich) were added to  
320 induce EBV lytic replication. Twelve hours post induction, medium was replaced with fresh RPMI 1640  
321 supplied with 10% FBS.

322 As for lymphocyte-origin EBV preparation, Akata-EBV cell strains were cultured in RPMI 1640 supplied  
323 with 5% FBS. Aliquot cells to the density of  $2 \times 10^6$ /mL, then goat-anti-human IgG (H0111-6-100ML,  
324 Tianfun Xinqu Zhenglong Biochem. Lab) was added to induce EBV lytic replication. Six-hours post  
325 induction, medium was replaced with fresh RPMI 1640 supplied with 5% FBS. For both preparation,  
326 three days post medium replacement, supernatant was collected, filtered, and centrifuged. Pellets which  
327 contained the virions were resuspended with RPMI 1640. Resuspended virions were frozen in liquid N<sub>2</sub>  
328 and then stored at -80 °C for further use.

### 329 **EBV in vitro infection analysis**

330 Epithelial cell lines were seeded in 96-well plates. Twenty-four hours later, virions with or without  
331 indicated concentration of sHLA-DR or sgp42 were prepared, incubated at 37 °C for an hour, and then  
332 added to cells. Twenty-four to 48 hours later, flow cytometry was applied to evaluate green fluorescence.  
333 For IC<sub>50</sub> fitting, the percentage of fluorescent positive cells were normalized by cells infected with  
334 virions without soluble proteins and dilution ratios were log<sub>10</sub> transformed before non-linear regression  
335 was applied. IC<sub>50</sub>s were fitted by Prism 9.

### 336 **In situ hybridization (ISH) and immunohistochemistry (IHC)**

337 The cases of atypical dysplasia in the nasopharynx were identified through the pathological station system  
338 in Sun Yat-sen University Cancer Center (SYSUCC) between January 2009 and April 2020. A total of 27  
339 cases of atypical dysplasia in nasopharynx with adequate formalin-fixed and paraffin-embedded (FFPE)  
340 specimens were collected for subsequent testing. The EBV probe in situ hybridization kit (ISH-7001,  
341 ZSGB-BIO) was used to detect EBERs in TMA slides, following the manufacturer's protocol.  
342 Immunohistochemistry was performed to analyze HLA-II expression using a benchmark ULTRA

343 automatic immunostaining device, with anti-HLA-DRA1 (diluted 1:600, ab92511-100ul; Abcam) as the  
344 primary antibody. The results were evaluated by two experienced pathologists who were blinded to the  
345 clinical data.

### 346 **Antibody**

347 Antibodies used in this study include the followings: anti-HLA-DRA1 (ab92511, Abcam), anti-HLA-  
348 DRB1 (ab133578, Abcam), anti- $\alpha$ -tubulin (2125S, CST), anti-rabbit IgG-HRP (31460, Thermo Fisher),  
349 anti-human IgG-HRP (ab6759, Abcam).

### 350 **Cell lines**

351 HEK293, and NP69 were maintained in a humidified atmosphere at 37 °C with 5% CO<sub>2</sub>. HEK293 was  
352 cultured in DMEM (11965092, Gibco) supplemented with 10% FBS (FSP500, ExCell Bio). NP69 was  
353 cultured in Keratinocyte SFM (1X) (17005042, Gibco). Details on the establishment of the HLA-II  
354 overexpressing cell lines refer to our previous study (17).

### 355 **Statistics**

356 For differences analysis of detected antibodies and neutralizing antibody titers, Wilcoxon or Kruskal-  
357 Wallis tests were applied for two or more stratifications of the characteristics. The continuous gp42-IgG  
358 titers were discretized according to the cutoffs based on the overall control groups, allowing for direct  
359 comparisons across different stratifications. Conditional logistic regression was applied for nested data  
360 analysis to estimate ORs and 95% CIs for the association between antibody and NPC risk stratified by  
361 time between baseline sampling and NPC diagnosis (<1 year, 1-5 years, and  $\geq 5$  years). No covariate is  
362 used to adjust OR. Categorical variables were treated as continuous variables in  $P_{\text{trend}}$  and  $P_{\text{heterogeneity}}$   
363 analyses. In terms of EBV infection rate differences under various circumstances, t-test is adopted since  
364 where residues complied normal distribution. All statistical analysis was done by R (4.3.1) and R  
365 packages (forestplot\_3.1.1, survminer\_0.4.9, survival\_3.5-520). A  $P$  value less than 0.05 was considered  
366 significant.

367 **Study approval**

368 This study has been conducted in accordance with the Declaration of Helsinki and the trial protocols were  
369 approved by the Ethics Review Committee of Sun Yat-sen University Cancer Center (YP2009051,  
370 B2020-362-01), Wuzhou Red Cross Hospital (LL2017-19), and Zhongshan City People’s Hospital  
371 (ZSKY2012(02)). This study is registered at Clinical Trials.gov (NCT00941538, NCT02501980) and  
372 Chinese Clinical Trial Registry (ChiCTR2000028776, ChiCTR2100041628). All participants signed the  
373 informed consent upon recruitment.

374 **Data availability**

375 Data of this study is available upon reasonable request from the corresponding authors.

376 **Author contributions**

377 M.-S.Z., S.-M.C., and X.-W.K. were responsible for conceptualization. M.-S.Z., S.-M.C., Y.-L.C., M.-F.J.,  
378 and X.-W.K. were responsible for methodology. X.-W.K., G.-L.B., Y.-H.H., Y.-F.K., Y.-C.L., X.Y., B.-  
379 H.W., Z.-Q.L., X.-C.C., S.-H.X., D.-F.L., T.L., S.-M.Y., R.-K.H., N.H., Q.-Y.W., Y.L., and A.Z. were  
380 responsible for investigation. X.-W.K., and H.C. were responsible for visualization. M.-S.Z., S.-M.C., Y.-  
381 L.C., and M.-F.J. were responsible for funding acquisition. M.-S.Z., S.-M.C., Y.-L.C., and M.-F.J.  
382 supervised the study. X.-W.K. wrote the original draft. M.-S.Z., S.-M.C., Y.-L.C., M.-F.J., Z.-W.L., Q.Z.,  
383 X.-M.H., and W.-M.Y. reviewed and revised the manuscript. The order of co-first authors was assigned by  
384 the contribution to this study.

385 **Acknowledgments**

386 This study was supported by Noncommunicable Chronic Diseases-National Science and Technology Major  
387 Project (2023ZD0501003), National Natural Science Foundation of China (82030046, 82073625,  
388 81860601, 82373655), Local Innovative and Research Teams Project of Guangdong Pearl River Talents

389 Program (2019BT02Y198), and Central Financial Transfer Payment Projects of the Chinese Government,  
390 Cancer Research Grant of Zhongshan City.

391 **List of supplementary materials**

392 Supplemental Figure 1 to 9

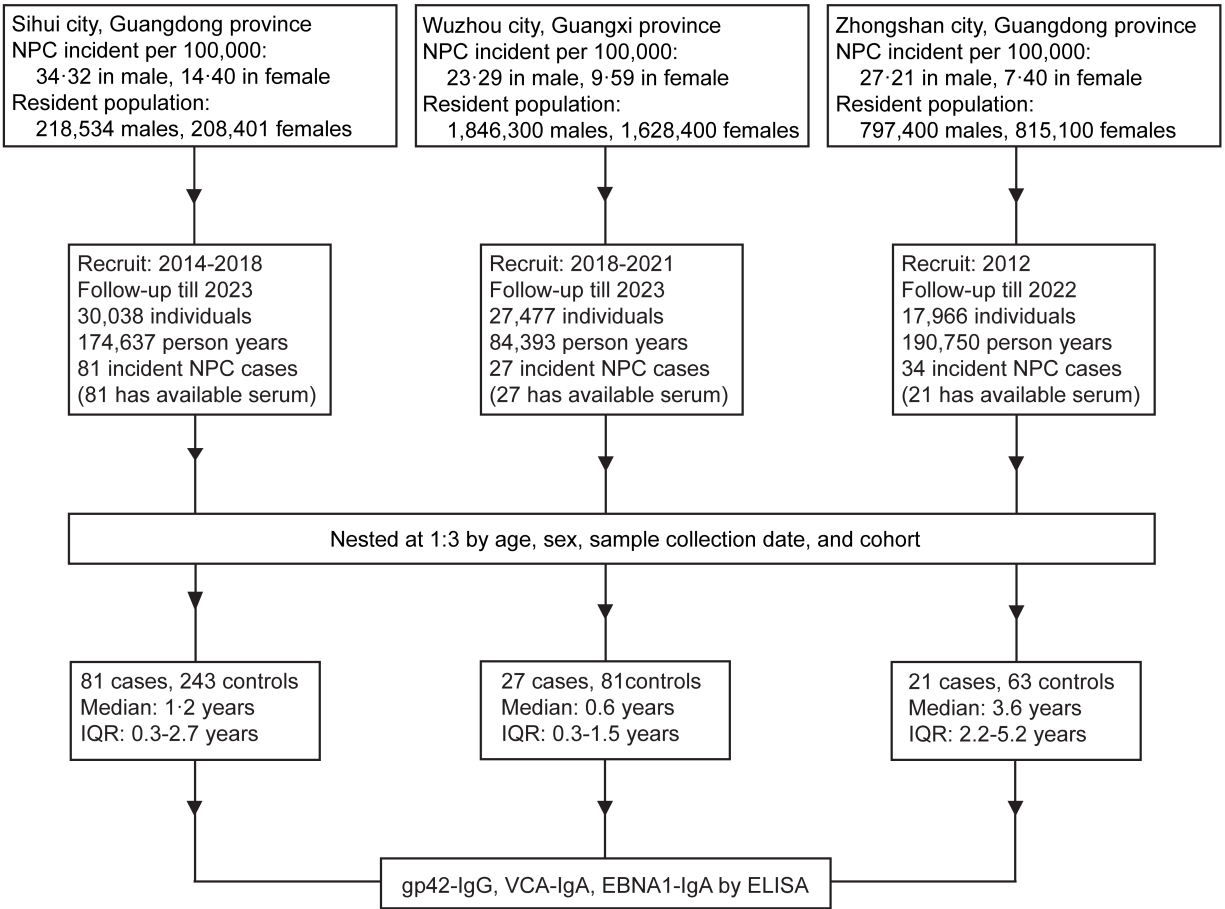
393 Supplemental Table 1 and 2

394

395 **References**

- 396 1. Chang ET, Ye W, Zeng YX, and Adami HO. The Evolving Epidemiology of Nasopharyngeal Carcinoma.  
397 *Cancer Epidemiol Biomarkers Prev.* 2021;30(6):1035-47.
- 398 2. National Cancer Center 2019 China Cancer Registry Annual Report. PEOPLE'S MEDICAL  
399 PUBLISHING HOUSE Co., LTD; 2021.
- 400 3. Chen YP, Chan ATC, Le QT, Blanchard P, Sun Y, and Ma J. Nasopharyngeal carcinoma. *Lancet.*  
401 2019;394(10192):64-80.
- 402 4. Hutt-Fletcher LM. EBV glycoproteins: where are we now? *Future Virol.* 2015;10(10):1155-62.
- 403 5. Haque T, Johannessen I, Dombagoda D, Sengupta C, Burns DM, Bird P, et al. A mouse monoclonal  
404 antibody against Epstein-Barr virus envelope glycoprotein 350 prevents infection both in vitro and in vivo.  
405 *J Infect Dis.* 2006;194(5):584-7.
- 406 6. Zhang X, Hong J, Zhong L, Wu Q, Zhang S, Zhu Q, et al. Protective anti-gB neutralizing antibodies  
407 targeting two vulnerable sites for EBV-cell membrane fusion. *Proc Natl Acad Sci U S A.*  
408 2022;119(32):e2202371119.
- 409 7. Zhu QY, Shan S, Yu J, Peng SY, Sun C, Zuo Y, et al. A potent and protective human neutralizing antibody  
410 targeting a novel vulnerable site of Epstein-Barr virus. *Nat Commun.* 2021;12(1):6624.
- 411 8. Snijder J, Ortego MS, Weidle C, Stuart AB, Gray MD, McElrath MJ, et al. An Antibody Targeting the  
412 Fusion Machinery Neutralizes Dual-Tropic Infection and Defines a Site of Vulnerability on Epstein-Barr  
413 Virus. *Immunity.* 2018;48(4):799-811 e9.
- 414 9. Cohen JI. Epstein-barr virus vaccines. *Clin Transl Immunology.* 2015;4(1):e32.
- 415 10. Coghill AE, Bu W, Nguyen H, Hsu WL, Yu KJ, Lou PJ, et al. High Levels of Antibody that Neutralize B-  
416 cell Infection of Epstein-Barr Virus and that Bind EBV gp350 Are Associated with a Lower Risk of  
417 Nasopharyngeal Carcinoma. *Clin Cancer Res.* 2016;22(14):3451-7.
- 418 11. Coghill AE, Bu W, Hsu WL, Nguyen H, Yu KJ, Chien YC, et al. Evaluation of Total and IgA-Specific  
419 Antibody Targeting Epstein-Barr Virus Glycoprotein 350 and Nasopharyngeal Carcinoma Risk. *J Infect*  
420 *Dis.* 2018;218(6):886-91.
- 421 12. Coghill AE, McGuire A, Sinha S, Homad L, Sinha I, Sholukh A, et al. Epstein-Barr Virus Glycoprotein  
422 Antibody Titers and Risk of Nasopharyngeal Carcinoma. *Open Forum Infect Dis.* 2022;9(12):ofac635.
- 423 13. Zhu QY, Kong XW, Sun C, Xie SH, Hildesheim A, Cao SM, et al. Association between Antibody  
424 Responses to Epstein-Barr Virus Glycoproteins, Neutralization of Infectivity, and the Risk of  
425 Nasopharyngeal Carcinoma. *mSphere.* 2020;5(6).
- 426 14. Hong J, Wei D, Wu Q, Zhong L, Chen K, Huang Y, et al. Antibody Generation and Immunogenicity  
427 Analysis of EBV gp42 N-Terminal Region. *Viruses.* 2021;13(12).
- 428 15. Jin S, Li R, Chen MY, Yu C, Tang LQ, Liu YM, et al. Single-cell transcriptomic analysis defines the  
429 interplay between tumor cells, viral infection, and the microenvironment in nasopharyngeal carcinoma. *Cell*  
430 *Res.* 2020;30(11):950-65.

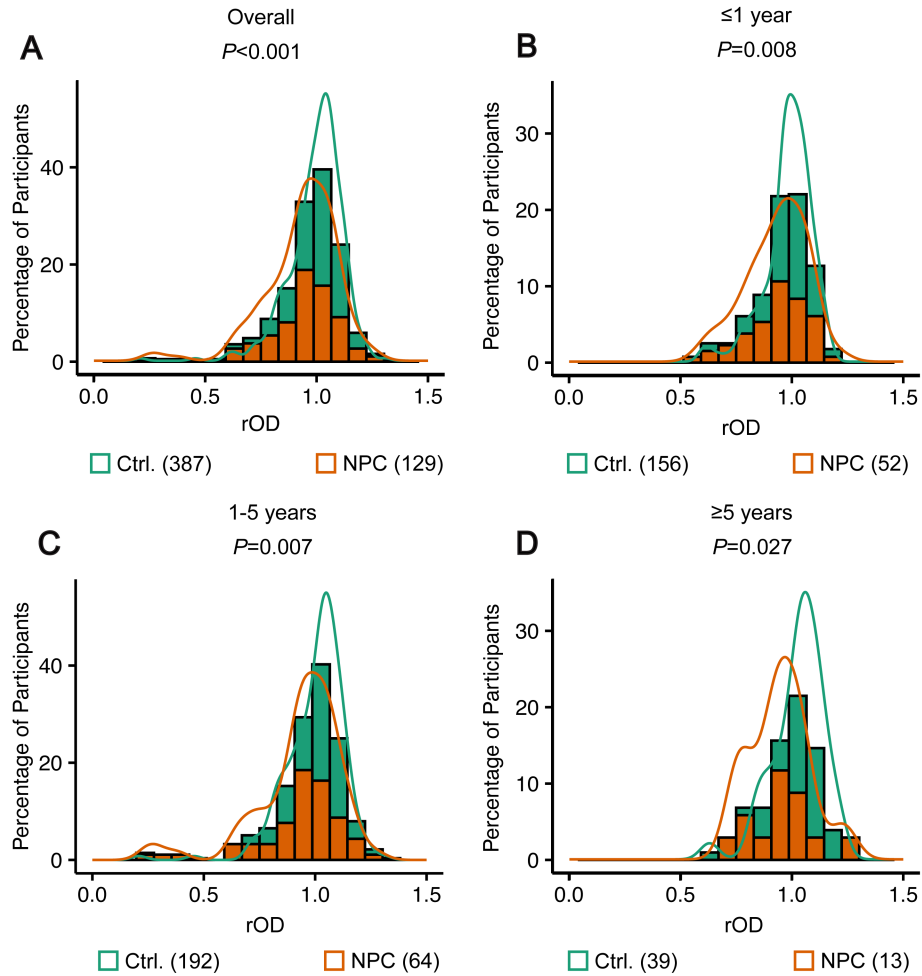
- 431 16. Tan LP, Tan GW, Sivanesan VM, Goh SL, Ng XJ, Lim CS, et al. Systematic comparison of plasma EBV  
432 DNA, anti-EBV antibodies and miRNA levels for early detection and prognosis of nasopharyngeal  
433 carcinoma. *Int J Cancer*. 2020;146(8):2336-47.
- 434 17. Zhao GX, Fang XY, Bu GL, Chen SJ, Sun C, Li T, et al. Potent human monoclonal antibodies targeting  
435 Epstein-Barr virus gp42 reveal vulnerable sites for virus infection. *Cell Rep Med*. 2024;5(5):101573.
- 436 18. Borza CM, and Hutt-Fletcher LM. Alternate replication in B cells and epithelial cells switches tropism of  
437 Epstein-Barr virus. *Nat Med*. 2002;8(6):594-9.
- 438 19. Woellmer A, and Hammerschmidt W. Epstein-Barr virus and host cell methylation: regulation of latency,  
439 replication and virus reactivation. *Curr Opin Virol*. 2013;3(3):260-5.
- 440 20. Chen GH, Liu Z, Yu KJ, Coghill AE, Chen XX, Xie SH, et al. Utility of Epstein-Barr Virus DNA in  
441 Nasopharynx Swabs as a Reflex Test to Triage Seropositive Individuals in Nasopharyngeal Carcinoma  
442 Screening Programs. *Clin Chem*. 2022;68(7):953-62.
- 443 21. Zheng XH, Wang RZ, Li XZ, Zhou T, Zhang JB, Zhang PF, et al. Detection of methylation status of  
444 Epstein-Barr virus DNA C promoter in the diagnosis of nasopharyngeal carcinoma. *Cancer Sci*.  
445 2020;111(2):592-600.
- 446 22. Jiang R, Scott RS, and Hutt-Fletcher LM. Epstein-Barr virus shed in saliva is high in B-cell-tropic  
447 glycoprotein gp42. *J Virol*. 2006;80(14):7281-3.
- 448 23. Hadinoto V, Shapiro M, Sun CC, and Thorley-Lawson DA. The dynamics of EBV shedding implicate a  
449 central role for epithelial cells in amplifying viral output. *PLoS Pathog*. 2009;5(7):e1000496.
- 450 24. Frangou P, Buettner M, and Niedobitek G. Epstein-Barr virus (EBV) infection in epithelial cells in vivo:  
451 rare detection of EBV replication in tongue mucosa but not in salivary glands. *J Infect Dis*.  
452 2005;191(2):238-42.
- 453 25. Wolf H, Haus M, and Wilmes E. Persistence of Epstein-Barr virus in the parotid gland. *J Virol*.  
454 1984;51(3):795-8.
- 455 26. Liu Z, Ji MF, Huang QH, Fang F, Liu Q, Jia WH, et al. Two Epstein-Barr virus-related serologic antibody  
456 tests in nasopharyngeal carcinoma screening: results from the initial phase of a cluster randomized  
457 controlled trial in Southern China. *Am J Epidemiol*. 2013;177(3):242-50.
- 458 27. Tholen DW, Kroll M, and Astles JR. *Evaluation of the linearity of quantitative measurement procedures a  
459 statistical approach; approved guideline*. Wayne, Pa., U.S.A: CLSI; 2003.
- 460 28. Andreasson U, Perret-Liaudet A, van Waalwijk van Doorn LJ, Blennow K, Chiasserini D, Engelborghs S,  
461 et al. A Practical Guide to Immunoassay Method Validation. *Front Neurol*. 2015;6:179.
- 462
- 463



464

465 **Figure 1. A Flow chart of study design.** A total 75,481 individuals from three independent prospective  
 466 cohorts established in three NPC epidemic regions (Sihui city, Guangdong province; Wuzhou city,  
 467 Guangdong province; Zhongshan city, Guangdong province) in southern China were recruited 2014 to 2018,  
 468 2018 to 2021, and 2012 years. A total of 129 serum-available incident NPC cases were identified until  
 469 2023 and each case matched to three controls from individual cohort by age, sex, sample collection dates.  
 470 Titers of gp42-IgG, VCA-IgA, and EBNA1-IgA were measured by ELISA.

471

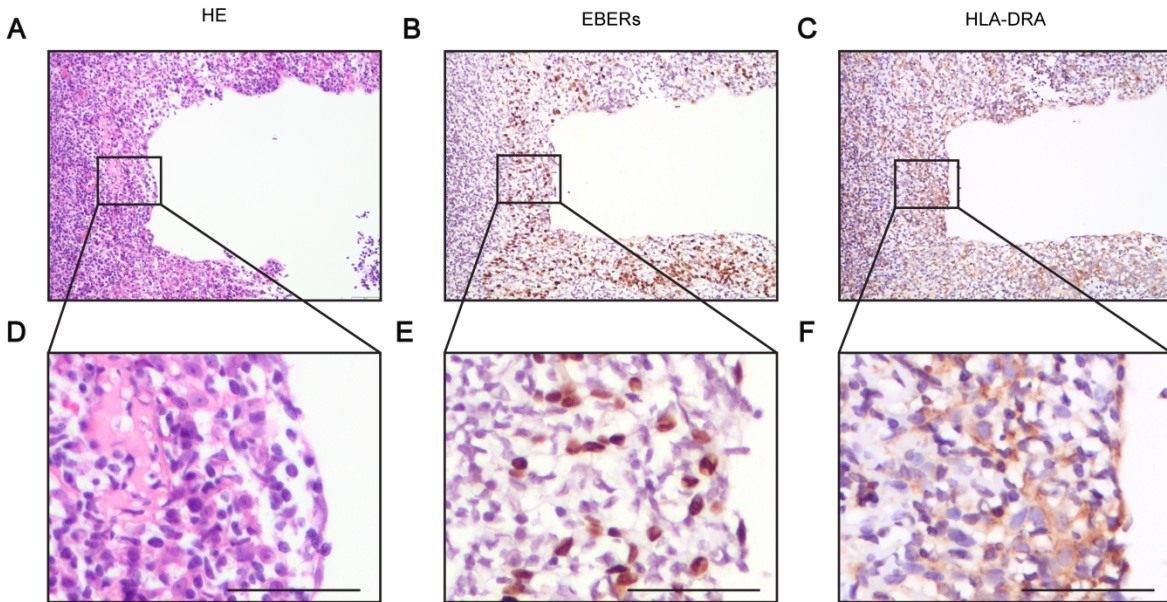


472

473 **Figure 2. Analysis of gp42-IgG levels in the nested case-control study.** Distributions of gp42-IgG  
 474 levels in (A) the overall cohort, (B) the cohort with follow-up duration  $\leq 1$  year, (C) the cohort with  
 475 follow-up duration 1-5 years, (D) the cohort with follow-up duration  $\geq 5$  years. rOD is a standardized  
 476 OD450-OD630 value, which was consistent across testing batches (Refer to Methods for details). The  
 477 lines at the top of each histogram represent kernel density estimations. Wilcoxon tests were used to  
 478 calculate  $P$  values, which are shown under the subtitles. Numbers in the legends refer to the numbers of  
 479 participants in each group.

480





481

482 **Figure 3. HLA-II expression in nasopharyngeal atypical dysplasia. (A and D) HE staining. (B and E)**  
 483 **In situ hybridization to detect EBERS. (C and F) Immunohistochemistry to detect HLA-DRA. Shown**  
 484 **was a representative out of 27 samples. A-C were shot at 20 $\times$ , D-F were zoomed in from the black square**  
 485 **region, and scale bars at lower right represent 50  $\mu$ m.**

486

**Table 1. Demographic characteristics of individuals in the nested case-control study.**

Characteristic	Follow-up periods before NPC onset							
	Overall		≤1 year		1-5 years		≥5 years	
	Control	Case	Control	Case	Control	Case	Control	Case
<b>Sex</b>								
Male	294 (76.0%)	98 (76.0%)	123 (78.8%)	41 (78.8%)	132 (68.8%)	44 (68.8%)	39 (100.0%)	13 (100.0%)
Female	93 (24.0%)	31 (24.0%)	33 (21.2%)	11 (21.2%)	60 (31.2%)	20 (31.2%)	0 (0.0%)	0 (0.0%)
<b>Age, years</b>								
<40	36 (9.3%)	12 (9.3%)	15 (9.6%)	5 (9.6%)	15 (7.8%)	5 (7.8%)	6 (15.4%)	2 (15.4%)
40-50	108 (27.9%)	36 (27.9%)	45 (28.8%)	15 (28.8%)	57 (29.7%)	19 (29.7%)	6 (15.4%)	2 (15.4%)
50-60	171 (44.2%)	57 (44.2%)	75 (48.1%)	25 (48.1%)	75 (39.1%)	25 (39.1%)	21 (53.8%)	7 (53.8%)
≥60	72 (18.6%)	24 (18.6%)	21 (13.5%)	7 (13.5%)	45 (23.4%)	15 (23.4%)	6 (15.4%)	2 (15.4%)
<b>Location</b>								
Sihui	243 (62.8%)	81 (62.8%)	105 (67.3%)	35 (67.3%)	120 (62.5%)	40 (62.5%)	18 (46.2%)	6 (46.2%)
Wuzhou	81 (20.9%)	27 (20.9%)	45 (28.8%)	15 (28.8%)	36 (18.8%)	12 (18.8%)	0 (0.0%)	0 (0.0%)
Zhongshan	63 (16.3%)	21 (16.3%)	6 (3.8%)	2 (3.8%)	36 (18.8%)	12 (18.8%)	21 (53.8%)	7 (53.8%)
<b>NPC risk score</b>								
Low	305 (78.8%)	21 (16.3%)	123 (78.8%)	5 (9.6%)	148 (77.1%)	11 (17.2%)	34 (87.2%)	5 (38.5%)
Medium	59 (15.2%)	23 (17.8%)	24 (15.4%)	2 (3.8%)	32 (16.7%)	18 (28.1%)	3 (7.7%)	3 (23.1%)
High	23 (5.9%)	85 (65.9%)	9 (5.8%)	45 (86.5%)	12 (6.2%)	35 (54.7%)	2 (5.1%)	5 (38.5%)

488 NPC, nasopharyngeal carcinoma; NPC risk score (P value) of each participant is determined by a risk  
 489 prediction algorithm ( $\text{Logit } P = -3.934 + 2.203 \times \text{VCA-IgA} + 4.797 \times \text{EBNA1-IgA}$ ) and the risks of NPC are  
 490 stratified as: low risk,  $P < 0.65$ ; medium risk,  $0.65 \leq P < 0.98$ ; high risk,  $P \geq 0.98$ .

492 **Table 2. Conditional logistic regression analysis reveals nasopharyngeal carcinoma risk associated**  
 493 **with gp42-IgG level across different follow-up periods.**

Follow-up periods	Cases (%)	Controls (%)	ORs (95% CIs)	<i>P</i> values
<b>Overall</b>				
<b>Quartile 1 (&lt;0.94)</b>	56 (43.4)	97 (25.1)	1	
<b>Quartile 2 (0.94-1.02)</b>	28 (21.7)	96 (24.8)	0.43 (0.24-0.76)	0.004
<b>Quartile 3 (1.02-1.07)</b>	24 (18.6)	97 (25.1)	0.36 (0.20-0.65)	0.001
<b>Quartile 4 (≥1.07)</b>	21 (16.3)	97 (25.1)	0.29 (0.15-0.55)	<0.001
<b>Per unit increase</b>			0.66 (0.54-0.81)	<0.001
<b>≤1 year</b>				
<b>Quartile 1 (&lt;0.94)</b>	24 (46.2)	37 (23.7)	1	
<b>Quartile 2 (0.94-1.02)</b>	11 (21.2)	56 (35.9)	0.25 (0.11-0.61)	0.002
<b>Quartile 3 (1.02-1.07)</b>	9 (17.3)	35 (22.4)	0.30 (0.11-0.81)	0.018
<b>Quartile 4 (≥1.07)</b>	8 (15.4)	28 (17.9)	0.33 (0.11-0.99)	0.048
<b>Per unit increase</b>			0.67 (0.47-0.96)	0.030
<b>1-5 years</b>				
<b>Quartile 1 (&lt;0.94)</b>	25 (39.1)	52 (27.1)	1	
<b>Quartile 2 (0.94-1.02)</b>	15 (23.4)	33 (17.2)	0.84 (0.36-1.98)	0.696
<b>Quartile 3 (1.02-1.07)</b>	13 (20.3)	53 (27.6)	0.46 (0.21-1.03)	0.058
<b>Quartile 4 (≥1.07)</b>	11 (17.2)	54 (28.1)	0.33 (0.13-0.84)	0.020
<b>Per unit increase</b>			0.68 (0.51-0.90)	0.007
<b>≥5 years</b>				
<b>Quartile 1 (&lt;0.94)</b>	7 (53.8)	8 (20.5)	1	
<b>Quartile 2 (0.94-1.02)</b>	2 (15.4)	7 (17.9)	0.32 (0.04-2.40)	0.266
<b>Quartile 3 (1.02-1.07)</b>	2 (15.4)	9 (23.1)	0.21 (0.03-1.69)	0.141
<b>Quartile 4 (≥1.07)</b>	2 (15.4)	15 (38.5)	0.05 (0.00-0.89)	0.042
<b>Per unit increase</b>			0.40 (0.18-0.90)	0.027

494 The quartile cutoffs based on the overall control groups, allowing for direct comparisons across different  
 495 stratifications. In the trend analysis, the values of discretized gp42-IgG were treated as continuous variable.